

Analytical results for a continuum model of crystalline tensionless surfaces. I. Variational mean field study

Esteban Moro^{†‡§} and Rodolfo Cuerno^{†||}

[†]Departamento de Matemáticas and Grupo Interdisciplinar de Sistemas Complicados, Universidad Carlos III de Madrid, Avda. Universidad 30, E-28911 Leganés, Spain

Abstract. We study analytically the equilibrium and near-equilibrium properties of a model of surfaces relaxing via linear surface diffusion and subject to a lattice potential. We employ the variational mean field formalism introduced by Saito for the study of the sine Gordon model. In equilibrium, our variational theory predicts a first order roughening transition between a flat low temperature phase and a rough high temperature phase with the properties of the linear molecular beam epitaxy equation. The study of a Gaussian approximation to the Langevin dynamics of the system indicates that the surface shows hysteresis when we continuously tune temperature. Out of equilibrium, this Langevin dynamics approach shows that the surface mobility can have different behaviours as a function of a driving flux. Some considerations are made regarding different dimensionalities and underlying lattices, and connections are drawn to related models or different approaches to the same model we study.

PACS numbers: 68.35.Rh, 64.60.Cn, 64.60.Ht, 81.10.Aj

Submitted to: *J. Phys. A: Math. Gen.*

1. Introduction

During the last decade, there have been great theoretical and experimental efforts to understand surface growth. This is due to possible applications, *e.g.*, to the production of thin films and, from the basic point of view, to the interesting examples growing surfaces provide of non-equilibrium statistical systems [1], in some cases with strong relation to relevant equilibrium systems [2]. A very important example is provided by the discrete Gaussian (dG) model, which describes the universal features of the equilibrium roughening transition of many surfaces [3]. This transition is in the Kosterlitz-Thouless (KT) class, and thus the model is related to other important models featuring a

[‡] Present address: Theoretical Physics Department, University of Oxford, 1 Keble Road, OX1 3NP, UK

[§] moro@thphys.ox.ac.uk

^{||} cuerno@math.uc3m.es

similar transition, such as the F model or the Coulomb gas [2, 3]. The dG model describes a surface minimizing surface area (to linear approximation), in which the surface height takes on integer values. Relaxing the latter condition leads to the sine-Gordon (sG) model for a real valued height field subject to surface tension and to a (lattice) potential favouring integer values of the field. The sG model is amenable to approximate analytic treatments [4, 5] which have allowed to develop a rather complete picture of the equilibrium roughening transition, and of the surface near-equilibrium properties as determined by Langevin dynamics [6] or kinetic Monte Carlo simulations [7].

There exist surface growth contexts, such as growth by molecular beam epitaxy (MBE), in which the most relevant relaxation mechanism taking place at the surface is surface diffusion [1]. This, in turn, can be modelled as a surface minimizing curvature, instead of surface area. In reference [8], the following stochastic equation was proposed to study the interplay of this mechanism with a lattice potential favouring integer height values, similarly to the sG model

$$\frac{\partial h}{\partial t} = F - \kappa \Delta^2 h(\mathbf{r}) - \frac{2\pi V_0}{a_\perp} \sin\left(\frac{2\pi h(\mathbf{r})}{a_\perp}\right) + \eta(\mathbf{r}, t). \quad (1)$$

In (1), $h(\mathbf{r}, t)$ is the surface height above (a two-dimensional) substrate position \mathbf{r} at time t ; Δ is the two dimensional Laplacian and κ , V_0 , and a_\perp are positive constants. F is also a constant representing, *e.g.*, a driving flux of particles inducing the system to grow. η is a Gaussian white noise with zero average and correlations $\langle \eta(\mathbf{r}, t) \eta(\mathbf{r}', t') \rangle = 2T \delta(\mathbf{r} - \mathbf{r}') \delta(t - t')$, with T being temperature (we consider a unit Boltzmann's constant, $k_B \equiv 1$). In equilibrium ($F = 0$), this equation governs the thermal fluctuations of a surface described by (the continuum limit of) the Hamiltonian

$$\mathcal{H} = \frac{\kappa}{2} \sum_i \left\{ \left[\sum_\delta (h_i - h_{i+\delta}) \right]^2 + V_0 \left[1 - \cos\left(\frac{2\pi h_i}{a_\perp}\right) \right] \right\}, \quad h_i \in \mathbb{R}. \quad (2)$$

where $i + \delta$ denotes a nearest neighbour to site i . In [8], numerical simulations of (1) showed an equilibrium roughening transition, similar to that in the sG model; namely, for temperatures below a critical value T_R the lattice potential is relevant and the surface is flat, whereas for temperatures higher than T_R the surface is rough. Out of equilibrium ($F \neq 0$), the surface mobility (to be defined below) behaves in different ways, depending on F and T . Although these simulations have been extended [9, 10], no analytical approach had been made to study this model. In this paper we take a first step in this direction and apply to model (1)-(2) a variational mean-field approach successfully applied by Saito [4] to the study of the sG model. In a subsequent paper we will refine this study by means of a dynamic renormalization group (RG) analysis of (1). The present paper is organized as follows. In section 2 we briefly review the relationship between (1)-(2) and related models for which approximate analytical and/or numerical results are available. In section 3 we study the equilibrium Hamiltonian (2) within the variational scheme of [4]. Section 4 is devoted to the approximate study of the Langevin

dynamics (1) within a Gaussian approximation for the probability distribution of the height. A discussion of the results obtained and our conclusions are found in section 5. Some computational details on the solution of self-consistent equations relevant to section 3 can be found in appendix 6.1, while appendix 6.2 discusses how the results are modified when considering the model on a triangular lattice (as opposed to the square lattice studied in the rest of the paper), and appendix 6.3 contains a discussion on results for substrate dimensions different from two.

2. Background

Crystal surfaces are often described within the solid-on-solid (SOS) approximation, in which the surface is characterized by a two-dimensional lattice height variable h_i with $h_i/a_\perp \in \mathbb{Z}$ and i being the square lattice position on a $L \times L$ dimensional substrate. Perhaps the simplest model is the discrete Gaussian model (dG) mentioned in the introduction, whose Hamiltonian is (we take a unit lattice constant)

$$\mathcal{H}_{\text{dG}} = \frac{\nu}{2} \sum_{i,\delta} (h_i - h_{i+\delta})^2, \quad h_i/a_\perp \in \mathbb{Z} \quad (3)$$

where ν is a positive constant. Due to the difficulty to handle analytically the discrete sums in (3), a continuum approximation is adopted introducing a potential that preserves the periodic symmetry in (3) and favours integer height values, leading to the sine-Gordon (sG) model (for reviews, see [2, 3])

$$\mathcal{H}_{\text{sG}} = \frac{\nu}{2} \sum_{i,\delta} (h_i - h_{i+\delta})^2 + \sum_i V_0 \left[1 - \cos \left(\frac{2\pi h_i}{a_\perp} \right) \right] \quad h_i \in \mathbb{R}. \quad (4)$$

Both models undergo a KT-type roughening transition at a finite temperature T_R^{sG} between a flat and a rough phase. In the flat phase the roughness $w^2 = (1/L^2) \sum_i (h_i - \bar{h})^2$ [where $\bar{h} = (1/L^2) \langle \sum_i h_i \rangle$] is finite and L -independent, while in the rough phase it diverges with the system size as $w^2 \sim \ln L$, *i.e.*, as if we take $V_0 = 0$ in (4). In the flat phase, the lattice potential dominates and imposes a finite correlation length ξ . For $T \geq T_R^{\text{sG}}$ the lattice potential becomes irrelevant, although it modifies [5] the value of the surface tension ν , and the correlation length diverges. Specifically, $\xi \sim \exp\{C(T_R^{\text{sG}} - T)^{-1/2}\}$ for $T \rightarrow T_R^{\text{sG}-}$.

As mentioned in the introduction, our aim is to study surfaces in which minimization of surface area is replaced by minimization of surface curvature, and we will thus replace model (4) by the Hamiltonian (2) proposed in [8]. Interestingly, in the context of two-dimensional melting, Nelson [11] proposed (on the triangular lattice) the so called Laplacian roughening model

$$\mathcal{H}_{\text{LR}} = \frac{\kappa}{2} \sum_i \left[\sum_\delta (h_i - h_{i+\delta}) \right]^2, \quad h_i/a_\perp \in \mathbb{Z}. \quad (5)$$

In equilibrium, numerical simulations and RG studies (see references in [12]) indicate that (5) displays two phase transitions, both in the KT universality class, with an

hexatic phase between the two transition temperatures. However, the conclusions of analytical and numerical work by other authors (see a review in [13]) seem to be that model (5) features only one first order phase transition. Note model (2) is a natural continuum approximation of (5) in the same spirit as the sG model is an approximation of the dG model. The numerical study [8] of Langevin dynamics (1) for (2) found an equilibrium continuous roughening transition between a flat phase and a rough phase in which $w^2 \sim L^2$, the same behaviour of the so called linear MBE equation [that obtained by setting $V_0 \equiv 0$ in (1)]. Nevertheless, since the lattice potential modifies the value of the (in principle zero) surface tension, the long distance behaviour of the high temperature phase of model (2) was expected to be the same as that in the sG model. In what follows we apply Saito's variational treatment to (2) and (1). In the case of the sG model, such mean field study [4] allows to obtain the exact value of the roughening temperature, and a rather approximate estimation of the divergence of the correlation length near T_R^{sG} . Thus we expect to obtain relevant information from this mean-field scheme.

3. Variational mean-field method: equilibrium problem

Following Saito [4], our main assumption is that the most relevant features of model (2) can be described by a simpler, solvable Hamiltonian:

$$\mathcal{H}_0 = \frac{T}{2} \sum_{\mathbf{q}} S^{-1}(\mathbf{q}) h(\mathbf{q}) h(-\mathbf{q}) \quad (6)$$

where $h(\mathbf{q})$ are the Fourier components of the height field

$$h(\mathbf{q}) = \frac{1}{L} \sum_j e^{i\mathbf{q} \cdot \mathbf{r}_j} h_j. \quad (7)$$

Here we consider periodic boundary conditions. Thus, $q_x = 2\pi n_x/L$ with $n_x = -(L-1)/2, \dots, L/2$ and a similar relation holds for q_y . Equation (6) defines a Gaussian Hamiltonian in which the values of $S(\mathbf{q})$ are L^2 free parameters. We will fix them by minimization of the variational free energy $\mathcal{F}_V \equiv \mathcal{F}_0 + \langle \mathcal{H} - \mathcal{H}_0 \rangle_0$, which is known to be an upper bound of the exact free energy \mathcal{F} of model (2) by the Bogoliubov thermodynamic inequality [2]

$$\mathcal{F} \leq \mathcal{F}_V \equiv \mathcal{F}_0 + \langle \mathcal{H} - \mathcal{H}_0 \rangle_0 \quad (8)$$

where \mathcal{F}_0 is the free energy of model \mathcal{H}_0 and $\langle \dots \rangle_0$ stands for the average with respect to the Boltzmann factor $e^{-\mathcal{H}_0/T}$.

Using the Hamiltonians (2) and (6) we obtain for the rhs of equation (8)

$$\begin{aligned} \frac{\mathcal{F}_V}{T} = & -\frac{1}{2} \sum_{\mathbf{q}} \ln 2\pi S(\mathbf{q}) + \frac{1}{2} \sum_{\mathbf{q}} [S_0^{-1}(\mathbf{q}) - S^{-1}(\mathbf{q})] S(\mathbf{q}) \\ & + \frac{L^2 V_0}{T} \left\{ 1 - \exp \left(-\frac{2\pi^2}{a_{\perp}^2} w^2 \right) \right\} \end{aligned} \quad (9)$$

where we have defined $S_0 = T/(\kappa\omega(\mathbf{q}))$ with $\omega(\mathbf{q}) = 16[\sin^2(q_x/2) + \sin^2(q_y/2)]^2$ and

$$w^2 = \frac{1}{L^2} \sum_j h_j^2 = \frac{1}{L^2} \sum_{\mathbf{q} \neq 0} S(\mathbf{q}) \quad (10)$$

(note that model (2) is symmetric under $h \rightarrow -h$ and thus, in equilibrium, $\bar{h} \equiv 0$). By minimizing \mathcal{F}_V with respect to the parameters $S(\mathbf{q})$, we find they have to verify

$$S^{-1}(\mathbf{q}) = S_0^{-1}(\mathbf{q}) + 4\pi^2 \frac{V_0}{a_\perp^2 T} \exp\left(-\frac{2\pi^2}{a_\perp^2} w^2\right). \quad (11)$$

We can rewrite (11) by noting that the second term on the rhs does not depend on \mathbf{q} . Hence

$$S(\mathbf{q}) = \frac{T}{\kappa(\omega(\mathbf{q}) + \xi^{-4})} \quad (12)$$

where ξ is a constant given by the self-consistent relation [note w^2 depends on ξ through (10) and (12)]

$$\kappa\xi^{-4} = \frac{4\pi^2 V_0}{a_\perp^2} \exp\left(-\frac{2\pi^2}{a_\perp^2} w^2\right). \quad (13)$$

Equations (12) and (13) are the solution to the equilibrium problem. We observe that the variational (Gaussian) approximation of Hamiltonian (2) has a structure factor $S(\mathbf{q})$ similar to that of the linear MBE equation. The only effect of the potential is to introduce a correlation length ξ given self-consistently by equations (13) and (12). Among all mathematical solutions of equation (13), the best approximation to model (2) is given by that value of ξ that minimizes the variational free energy \mathcal{F}_V , which we denote by ξ_{phys} . Note all roots of equation (13) can be easily shown to be stationary points of the function $\mathcal{F}_V(\xi)$.

In order to proceed analytically, we need to take the continuum limit of the integrals appearing in (9), (10). In this limit, we make the replacement $L^{-2} \sum_{\mathbf{q}} \rightarrow (2\pi)^{-2} \int d\mathbf{q}$, and we can approximate $\omega(\mathbf{q}) = \mathbf{q}^4$, hence using equation (12) we get

$$w^2 \simeq \frac{1}{(2\pi)^2} \int d\mathbf{q} \frac{T}{\kappa(\omega(\mathbf{q}) + \xi^{-4})} = \frac{T\xi^2}{8\kappa} - \frac{T}{4\kappa\pi^3} + \mathcal{O}(\xi^{-4}). \quad (14)$$

Keeping the dominant term in the above equation (in powers of ξ), and defining $x = 2\kappa^{1/2} a_\perp T^{-1/2} \pi^{-1} \xi^{-1}$ equation (13) becomes

$$x^4 = \gamma e^{-1/x^2} \quad (15)$$

where $\gamma = 64V_0 a_\perp^2 \kappa T^{-2} \pi^{-2}$. As shown in appendix 6.1, there are different solutions of equation (15) depending on γ (and therefore on temperature). Thus, $\xi^{-1} = 0$ is always a solution of (15), and is the unique solution for $T > T_C = 16V_0^{1/2} \kappa^{1/2} a_\perp / e\pi$. However, for $T \leq T_C$ there appear two other finite solutions $0 < \xi_1^{-1} < \xi_2^{-1}$ of equation (15). In order to check which of the three roots provides ξ_{phys} in this temperature range, we compute the free energy difference

$$\frac{\Delta\mathcal{F}_V(\xi)}{TL^2} \equiv \frac{1}{TL^2} [\mathcal{F}_V(\xi) - \mathcal{F}_V(\xi^{-1} = 0)] \simeq \frac{\xi^{-2}}{16} - \frac{V_0}{T} e^{-T\pi^2 \xi^2 / (4\kappa a_\perp^2)} + \mathcal{O}(\xi^{-4}). \quad (16)$$

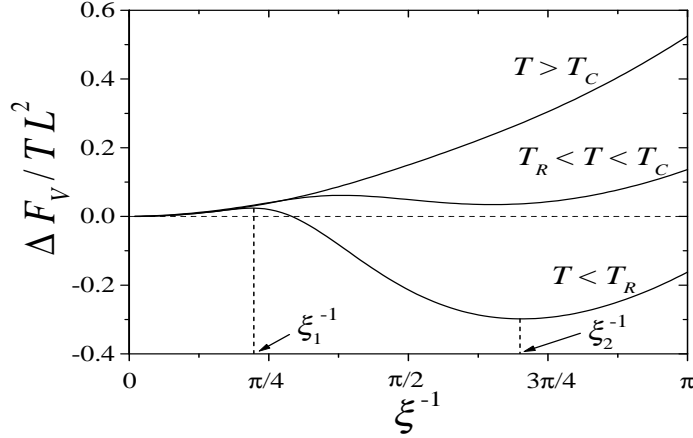


Figure 1. Variational mean free energy difference $\Delta\mathcal{F}_V$ as a function of the (inverse of the) correlation length for different temperatures. The values of ξ_1 and ξ_2 are only displayed for the $T < T_R$ case. The physical value of the correlation length ξ_{phys} is given by the global minimum of $\Delta\mathcal{F}_V$. For temperatures $T > T_R$ the global minimum is always reached at $\xi^{-1} = 0$. Parameters used are: $V_0 = a_{\perp} = \kappa = 1$.

We plot $\Delta\mathcal{F}_V(\xi)$ in figure 1 for different values of T . For $T \leq T_C$, as can be seen in the figure, $\Delta\mathcal{F}_V(\xi)$ has indeed a local maximum at ξ_1^{-1} and a local minimum at ξ_2^{-1} , while for $T > T_C$ both disappear. As derived in appendix 6.1, for temperatures above $T_R = (e^{1/2}/2)T_C \simeq 0.82T_C$, the variational free energy difference has its global minimum at $\xi_{\text{phys}}^{-1} = 0$. However, for lower temperatures $T < T_R$, the finite correlation length ξ_2 features a lower value of the variational free energy than the infinite correlation length solution, hence $\xi_{\text{phys}} = \xi_2$ in this temperature range. Summarizing, within the variational approximation a roughening transition takes place at a temperature

$$T_R = \frac{8}{\pi e^{1/2}} a_{\perp} \kappa^{1/2} V_0^{1/2}. \quad (17)$$

Above T_R the correlation length is infinite and the surface is rough, with the same properties as the linear MBE model, i.e. $S(\mathbf{q}) \sim \mathbf{q}^4$ and $w^2 \sim L^2$. Below T_R the surface is flat with a finite correlation length equal to ξ_2 . When we approach the roughening temperature from below, the correlation length does *not* diverge but, rather, tends to a constant value (see appendix 6.1) given by

$$\xi(T \rightarrow T_R^-) = \left(\frac{4\kappa a_{\perp}^2}{T_R \pi^2} \right)^{1/2} \quad (18)$$

implying the roughening transition at T_R is of first order. Specifically, a cusp develops in the free energy \mathcal{F}_V as a function of temperature at $T = T_R$, as depicted in figure 2.

Although the results in this section have been obtained using a certain continuum approximation, we have numerically verified all our conclusions using the exact discrete sums in (9) and (10). The exact variational results for the correlation length and the values of T_C and T_R for $L = 1024$ are compared in figure 2 to the approximate analytical expressions obtained in this section. We see that a first order transition indeed takes

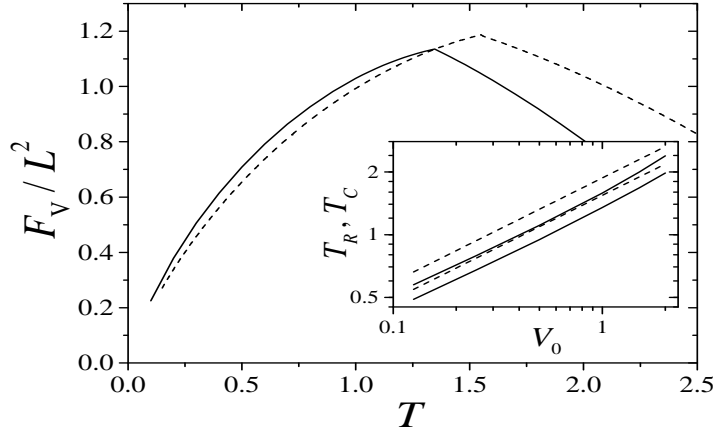


Figure 2. Variational free energy \mathcal{F}_V as a function of temperature for model (2) using the exact expression (9) (solid line) and our continuum approximation (dashed line). In both cases, \mathcal{F}_V develops a cusp at $T = T_R$ due to the jump in the physical value of ξ . Inset shows the values of T_R (lower curves) and T_C as functions of V_0 within our continuum approximation (dashed lines) and using the exact discrete expressions (solid lines). In both cases, $T_R \propto T_C \sim V_0^{1/2}$. Parameters used are $a_\perp = \kappa = 1$.

place, although the values of T_R and T_C are modified. However, we still observe the non-linear dependence of T_R on V_0 , see inset of figure 2.

4. Dynamics within the Gaussian approximation

In this section, we study the near-equilibrium dynamics of model (2) by means of the generalized Langevin growth equation

$$\frac{\partial h_i(t)}{\partial t} = F - \frac{\delta \mathcal{H}}{\delta h_i(t)} + \eta_i(t) \quad (19)$$

where $\eta_i(t)$ is a white noise with correlations $\langle \eta_i(t) \eta_j(t') \rangle = 2T \delta_{ij} \delta(t - t')$ and F is the flux of incoming particles in the surface growth picture, or a chemical potential difference in a generic context. This equation describes not only the non-equilibrium statistical dynamics of our model, but also the dynamics of the system fluctuations around the equilibrium state (for $F = 0$). Our approximation [4] to the study of equation (1) will be to assume a Gaussian time-dependent probability distribution for the height field. Thus, we only have to calculate the first two moments of the probability distribution, namely the mean height $\P \bar{h} = \langle h_i(t) \rangle$ and the second moment $\langle h(\mathbf{q}, t) h(-\mathbf{q}, t) \rangle = S(\mathbf{q}, t)$. Using equations (2) and (19) (see a detailed account in [14]) we find

$$\frac{d\bar{h}}{dt} = F - \frac{2\pi V_0}{a_\perp} \left\langle \sin \left(\frac{2\pi h_i}{a_\perp} \right) \right\rangle \quad (20)$$

$$\frac{dS(\mathbf{q}, t)}{dt} = -2TS(\mathbf{q}, t) \left[S_0^{-1}(\mathbf{q}) - S^{-1}(\mathbf{q}, t) + \frac{4\pi^2 V_0}{a_\perp^2 T} \left\langle \cos \left(\frac{2\pi h_i}{a_\perp} \right) \right\rangle \right] \quad (21)$$

\P We make the homogeneity assumption that $\langle h_i(t) \rangle$ is independent of substrate position, see [4].

$$= -4TS(\mathbf{q}, t) \frac{\delta \mathcal{F}_V}{\delta S(\mathbf{q}, t)}$$

where, within our Gaussian approximation,

$$\left\langle \sin \left(\frac{2\pi h}{a_\perp} \right) \right\rangle = e^{-2\pi^2 w^2(t)/a_\perp^2} \sin \left(\frac{2\pi \bar{h}}{a_\perp} \right) \quad (22)$$

$$\left\langle \cos \left(\frac{2\pi h}{a_\perp} \right) \right\rangle = e^{-2\pi^2 w^2(t)/a_\perp^2} \cos \left(\frac{2\pi \bar{h}}{a_\perp} \right) \quad (23)$$

with $w^2(t)$ being the time dependent surface roughness. In all cases, we will study the set of coupled differential equations (20) and (21) subject to the initial condition $h_i(t=0) = 0$ for all substrate positions i .

4.1. Equilibrium

In equilibrium, i.e. for $F = 0$, the solution of equation (20) is $\bar{h} = 0$ [note (22)] and the solution of (21) is the same as that of (11) and (13) obtained in the previous section. The interest of equation (21) is that it allows us to study dynamically how does the system choose the physical value of the correlation length, and corroborate the results obtained in the previous section from the point of view of Langevin dynamics. Thus, we will integrate numerically the complete set of L^2 discrete equations (20) and (21) and perform the following experiment: starting from a flat surface and $T = 0$, we increase temperature by a certain (small) amount and wait until the system reaches equilibrium. Then, we increase temperature by the same amount and repeat the equilibration process. When the temperature is high enough (i.e. once the system is in the rough phase) we decrease temperature by the same amount and repeat the process of equilibration until $T = 0$ is reached back closing a temperature cycle.

We observe that the equilibrium first order transition found in the previous section indeed induces hysteresis in the system correlation length (see figure 3) when the system is heated starting from $T = 0$, in the sense that the roughening transition takes place at the *higher* temperature T_C and *not* at T_R . The reason is that, for all T up to T_C , the system stays in the local \mathcal{F}_V minimum at ξ_2 , even though for $T_R < T < T_C$ the free energy already has its global minimum at $\xi^{-1} = 0$, since there is an energy barrier for the system to jump across the local maximum in $\Delta \mathcal{F}_V$. Once the local minimum at ξ_2 disappears (i.e. for $T \geq T_C$), the surface is rough and exhibits an infinite correlation length. Conversely, when the system is cooled down starting at $T > T_C$, the system remains in the rough phase until $T = 0$ is reached because $\xi^{-1} = 0$ is always a free energy minimum.

4.2. Non-equilibrium

In this section we allow $F \neq 0$ in (20) and (21), in which case the former no longer has the trivial solution ($\bar{h} = 0$). Rather, when the flux F is small (quasi-equilibrium condition) we expect the system to feature a structure factor $S(\mathbf{q}, t)$ of the same form as in

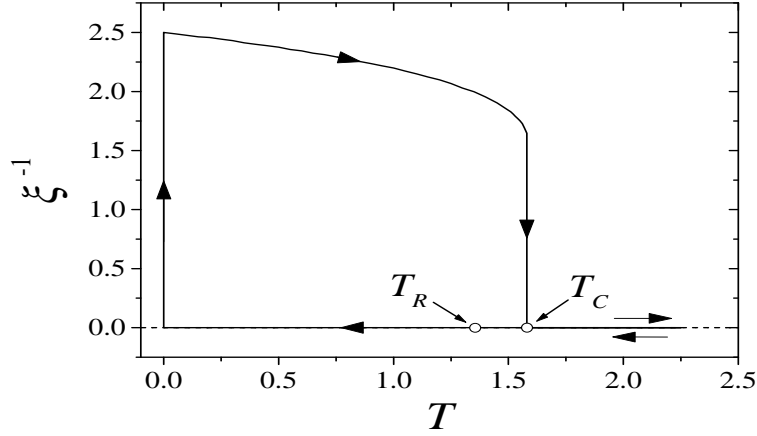


Figure 3. (Inverse of the) physical correlation length as a function of temperature, as determined from equations (21) and (12). The arrows indicate the heating and cooling experiment explained in the text. Parameters used are $V_0 = a_\perp = \kappa = 1$ and $L = 1024$.

equilibrium, all non-equilibrium effects reflecting in the (possibly non-trivial) behaviour of the average height. Actually, numerical simulations [8, 9] of the full non-linear model (1) seem to confirm this expectation. For this reason we neglect the feedback effect of the evolution of $\bar{h}(t)$ on the structure factor $S(\mathbf{q}, t)$ and take

$$S(\mathbf{q}, t) \simeq \frac{k_B T}{\kappa(\omega(\mathbf{q}) + \xi^{-4})} \quad (24)$$

where ξ is given by the physical equilibrium solution of section 3. Within this approximation, $F_c(T) \equiv \frac{2\pi V_0}{a_\perp} \exp\{-2\pi^2 w^2/a_\perp^2\}$ becomes a constant and equation (20) can be written as

$$\frac{d\bar{h}}{dt} = F - F_c \sin \frac{2\pi\bar{h}}{a_\perp} \quad (25)$$

which is simple to integrate analytically (exact expressions for the solution can be found in [4] and [14]). This equation has two different solutions depending on the values of F . If $F \leq F_c$, then \bar{h} tends to a constant value and the surface does not grow. If we define the surface mobility μ as

$$\mu = \frac{1}{F} \overline{\left\langle \frac{d\bar{h}}{dt} \right\rangle} \quad (26)$$

where the overline stands for average over a time larger than μ^{-1} , then for $F > F_c$ one obtains from the exact solution of (25) a non-zero value for μ :

$$\mu = \left(1 - \frac{F_c^2}{F^2}\right)^{1/2}. \quad (27)$$

In figure 4 we plot the surface mobility as a function of T . Using the equilibrium solution for ξ described in section 3, for temperatures above roughening ($T > T_R$), we have that $\xi_{\text{phys}}^{-1} = 0$, which implies $F_c = 0$ and $\mu = 1$. Thus, above roughening the surface shows linear growth with a maximum (unit) mobility. In the flat phase ($T < T_R$) the

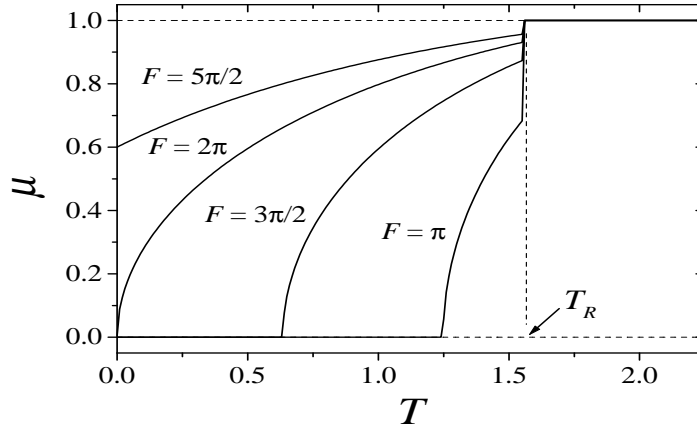


Figure 4. Surface mobility as a function of T for different values of the driving flux F . The values of the mobility are obtained from equation (26) using equations (12) and (13) with the parameter values $V_0 = \kappa = a_\perp = 1$.

mobility is equal to zero (i.e. the surface does not move) for a small flux $F < F_c(T)$. For larger values of the flux ($F > F_c(T)$), the mobility depends nonlinearly on T for all temperatures up to T_R . Due to the jump of the correlation length at $T = T_R$, the mobility also has a jump at this temperature value. These three behaviours of the surface mobility as a function of temperature and driving flux agree with those obtained [8, 9] for the full model (1), except for the discrete jump of μ at $T = T_R$.

5. Discussion and conclusions

Summarizing the equilibrium results obtained in the previous sections, the variational approximation predicts a first order phase transition for model (2), and the associated hysteresis phenomenon. In particular, within a Gaussian approximation, Langevin dynamics predicts that a rough surface can preserve its infinite correlation length when cooled down across the roughening temperature. Moreover we have found that these results apply both on the square and on the triangular lattices (see appendix 6.2). Hysteresis behaviour and a first order transition have been reported in [15] and [16] for models related with the Laplacian roughening (LR) model (5) on the square lattice and for the LR model on the triangular lattice [17]. However, as mentioned in the introduction, other authors seem to obtain two KT transitions for the LR model both on the square [18] and on the triangular [19] lattices. Note that our Langevin dynamics results within the Gaussian approximation yield a discrete jump in the surface mobility μ at T_R , which is not found in simulations of the full nonlinear model (1). This might indicate that the first order character of the transition is in our case an artifact of the variational approximation. Moreover, this approximation (see appendix 6.3) also predicts a phase transition for model (2) in $d = 1$, which is also obtained for the sG model. This result points out the limitations of this approximate framework for

situations in which fluctuations are very relevant for the system behaviour (as in the $d = 1$ case). Since model (2) features intrinsically strong fluctuations (as does *e.g.* the linear MBE equation [1]), it is desirable to go beyond our present mean field approach to this model. We can take two steps in this direction. One (numerical) is to perform extended simulations of both the LR model and model (2) [or, equivalently, its equilibrium Langevin dynamics (1)]. The results [10] seem to indicate that in *both* cases there is only one continuum transition, though with strong size dependence in the LR case for sizes up to moderate (but not large). The other (analytical) improvement is to perform a dynamic RG analysis of (1) along the lines of [5] for the sG model. This study is particularly important bearing in mind that the lattice potential is expected to contribute a surface tension, absent in equation (1), which should then dominate the scaling behaviour as compared with surface diffusion [1]. This phenomenon is clearly beyond our mean-field approach, which neglects parameter renormalization. Moreover, comparing with the sG case, in the latter the variational mean field [4] and the perturbative (in powers of V_0) RG [5] approaches yield the *same* (exact) roughening temperature $T_R^{\text{sG}} = 2\nu a_\perp^2/\pi$, which is independent of V_0 . However, in our case T_R does depend on the lattice potential (and on κ) as a fractional power. Thus, we do not expect a perturbative RG treatment to quantitatively agree with the expression for T_R derived here. This will be the subject of a forthcoming publication.

Acknowledgments

The authors are pleased to thank Angel Sánchez for discussions, encouragement and a detailed reading of the manuscript. This work has been partially supported by DGES grant No. PB96-0119.

6. Appendix

6.1. Solution of the self-consistent equations

In this Appendix we calculate the self-consistent solution of equations (12) and (13) for the equilibrium correlation length of the variational approximation (6) to model (2). By defining $x = 2\kappa^{1/2}a_\perp T^{-1/2}\pi^{-1}\xi^{-1}$ and $\gamma = 64V_0a_\perp^2\kappa T^{-2}\pi^{-2}$, equations (12) and (13) become, within the continuum approximation made in section 3

$$x^4 = \gamma e^{-1/x^2}. \quad (28)$$

It is obvious that equation (28) always has the solution $x = 0$, and that for some values of γ it may also have non-zero solutions. Our first aim is to determine the critical value of γ for which $x = 0$ is the unique solution. To this end, we rewrite the equation in the following way

$$x = \gamma^{1/4} e^{-1/4x^2}. \quad (29)$$

Now the solutions are the intersections of the function $y = f(x) = \gamma^{1/4} e^{-1/4x^2}$ with the straight line $y = x$. As we can see in figure 5, for $\gamma > \gamma_C$ there are three solutions of

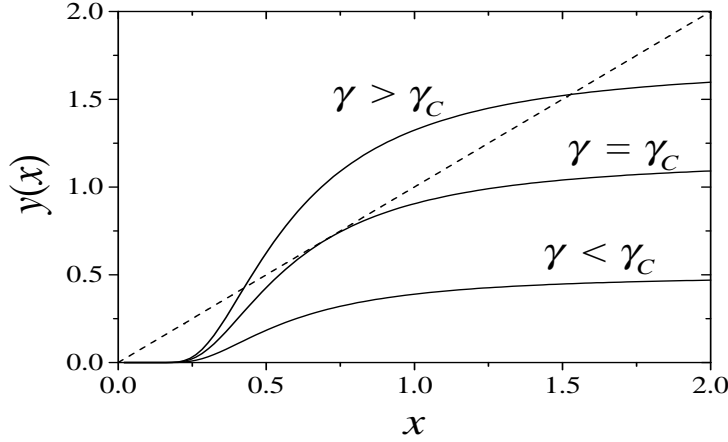


Figure 5. Graphical representation of equation (29). The dashed line is the $y = x$ function, while the solid lines show $y = \gamma^{1/4}e^{-1/4x^2}$ for different values of γ .

equation (29), two solutions for $\gamma = \gamma_C$ and only the trivial solution $x = 0$ for $\gamma < \gamma_C$. The value of γ_C can be calculated using that for $\gamma = \gamma_C$ the unique solution $x = x_s \neq 0$ verifies (29) and also the equation

$$1 = \gamma_C^{1/4} \frac{1}{2x_s^3} e^{-1/4x_s^2} \quad (30)$$

obtained by requiring that the slopes of $y = x$ and $y = f(x)$ be equal at $x = x_s$. With these two equations it is easy to obtain $x_s = 2^{-1/2}$ and $\gamma_C = e^2/4$. Using the definition of γ , the temperature for which $\xi^{-1} = 0$ is the only solution of equation (13) is then given by

$$T_C = \frac{16V_0^{1/2}\kappa^{1/2}a_{\perp}}{e\pi}. \quad (31)$$

Now, for $T < T_C$ we have to determine which of the three solutions of (28) provides the physical correlation length. Since $\xi^{-1} = 0$ is the unique solution for high temperatures, we take as a reference value $\mathcal{F}_V(\xi^{-1} = 0)$, and note that $\Delta\mathcal{F}(\xi) = \mathcal{F}_V(\xi) - \mathcal{F}_V(\xi^{-1} = 0)$ is stationary at any root of equation (13). Thus, we will consider as the physical solution for the correlation length that root of (13) for which \mathcal{F}_V has an absolute minimum. Starting out with high temperatures, the condition $\Delta\mathcal{F}_V(\xi) = 0$ will signal the temperature at (and below) which $\xi^{-1} = 0$ ceases to be the global minimum of the variational free energy and thus the system physical correlation length. Using our previous notation, the condition $\Delta\mathcal{F}_V(\xi) = 0$ reads

$$x^2 = \gamma' e^{-1/x^2} \quad (32)$$

where $\gamma' = 64\kappa a_{\perp}^2 V_0 / (\pi^2 T^2)$. Using the same argument as above, it is easy to show that for $\gamma' < \gamma'_R = e$ there are non-zero solutions of (32). This means, using the definition of γ' , that there is a temperature given by

$$T_R = \frac{e^{1/2}}{2} T_C, \quad (33)$$

such that for $T < T_R$ the global minimum of the free energy is attained for a correlation length $\xi \neq 0$, whereas for $T \geq T_R$ the physical solution is $\xi_{\text{phys}}^{-1} = 0$.

6.2. Triangular lattice

The Laplacian roughening model was initially proposed by Nelson on the triangular lattice [11]. Thus, it is worth studying how do the features of our model (2) change when the substrate geometry is different from the square lattice considered in the text. Nevertheless, we expect that only nonuniversal quantities —such as the transition temperature and the numerical value of correlation length— depend upon the lattice geometry. The Laplacian roughening model on the triangular lattice is given by

$$\mathcal{H}_{\text{LR}} = \frac{\kappa}{2} \sum_i \left[\sum_{\delta} (h_i - h_{i+\delta}) \right]^2 \quad (34)$$

with $i + \delta$ being any of the six nearest neighbours of site i . For this case [14], $\omega(\mathbf{q}) = 16\{\sin^2(q_x/2) + \sin^2[(q_x + \sqrt{3}q_y)/4] + \sin^2[(q_x - \sqrt{3}q_y)/4]\}^2$, where $\mathbf{q} = (n_x/L)\mathbf{b}_x + (n_y/L)\mathbf{b}_y$, with $\mathbf{b}_x = 2\pi[\mathbf{e}_x - (1/\sqrt{3})\mathbf{e}_y]$ and $\mathbf{b}_y = (4\pi/\sqrt{3})\mathbf{e}_y$, where $n_i = -(L-1)/2, \dots, L/2$ and \mathbf{e}_i are the standard basis vectors. In the continuum limit, $S_0(\mathbf{q}) \simeq 4T/(9\kappa\mathbf{q}^4)$, and we recover equation (13). Taking the continuum limit (i.e. $\frac{1}{L^2} \sum_{\mathbf{q}} \rightarrow \frac{\sqrt{3}}{2} \int_{BZ} \frac{d^2\mathbf{q}}{(2\pi)^2} \simeq \frac{\sqrt{3}}{4\pi} \int_0^{(2/\sqrt{3})^{1/2}\pi} q dq$, where BZ denotes the first Brillouin zone), we get

$$w^2 \simeq \frac{T}{2\pi\kappa(2/\sqrt{3})^2} \int_0^\pi \frac{q'}{q'^4 + \frac{\xi^{-4}}{(2/\sqrt{3})^2}} dq'. \quad (35)$$

Thus, by defining $T' = T/3$, and $\xi' = 3^{1/4}\xi$, we get the same equation (15) but with redefined constants T' and ξ' . One can readily reproduce all the results obtained in the text, simply by making the replacements $T \rightarrow T'$ and $\xi \rightarrow \xi'$. In conclusion, on the triangular lattice a first order roughening transition is also obtained, the only effect of the geometry being a shift in the value of the roughening temperature $T_R^{\text{triang.}} = T_R^{\text{square}}/3$.

6.3. Substrate dimensions $d \neq 2$

In this appendix we discuss the possibility to find a roughening transition in equilibrium when model (2) is defined on a substrate of generic dimension d . In that case, equation (13) is still valid, but with

$$w^2(\xi) \simeq \int \frac{d^d\mathbf{q}}{(2\pi)^d} \frac{T}{\kappa(\omega(\mathbf{q}) + \xi^{-4})}, \quad (36)$$

within the continuum limit. For substrate dimension $d > 4$, the integral (36) is finite for $\xi^{-1} = 0$, namely $w^2(\xi^{-1} = 0) = K_d \pi^{d-4} T / [\kappa(d-4)]$ (where K_d is the d -dimensional angular integral $K_d = \int d^{d-1}\Omega / (2\pi)^d = 2\pi^{d/2} / [(2\pi)^d \Gamma(d/2)]$). Thus, $\xi^{-1} = 0$ is no longer a solution of equation (13). Therefore the system has no rough solution and is

in the flat phase for all temperatures. On the other hand, for $d < 4$, the integral above may be approximated by

$$w^2(\xi) \lesssim \frac{T}{\kappa} \frac{\pi K_d}{4 \sin(\pi d/4)} \xi^{4-d}. \quad (37)$$

In this case, $\xi^{-1} = 0$ is always solution of equation (13), there being two additional finite solutions when $T < T_C^d$. The value of T_C^d can be calculated using the same argument as in $d = 2$ and is

$$T_C^{d<4} = \frac{8\kappa a_\perp^2 \sin(d\pi/4)}{(4-d)K_d e \pi^3} \left(\frac{4\pi^2 V_0}{\kappa a_\perp^2} \right)^{\frac{4-d}{4}}. \quad (38)$$

In order to know which solution of equation (13) minimizes the variational free energy, we calculate $\Delta\mathcal{F}_V$, which now reads

$$\frac{\Delta\mathcal{F}_V(\xi)}{TL^d} \simeq \frac{4-d}{d} \frac{\pi K_d}{8 \sin(\pi d/4)} \xi^{-d} - \frac{V_0}{T} e^{-2\pi^2 w^2/a_\perp^2}. \quad (39)$$

In this case, the local minimum $\xi_2^{-1} \neq 0$ is also the global minimum and the physical solution for temperatures below the roughening temperature ($T < T_R^{d<4}$), which is given by

$$T_R^{d<4} = \frac{d}{4} e^{\frac{4-d}{4}} T_C^{d<4}. \quad (40)$$

For temperatures above roughening ($T \geq T_R^{d<4}$), $\xi^{-1} = 0$ provides the global free energy minimum. Thus, for $d < 4$ there is a first order roughening transition at $T_R^{d<4}$. Note this includes $d = 1$, which might seem conflictive since in this case model (2) is expected to be in the rough phase for all values of T [11]: In $d = 1$ thermal fluctuations are expected to destroy the ordered flat phase for any temperature value. Our result can be understood by noting that \mathcal{F}_V is *not* a true free energy, in the sense that it is not the free energy of any model⁺, but rather an upper bound for the free energy of model (2). Actually, one obtains exactly the same result in the variational study of the sG model in $d = 1$ [4]. Note that in this reference the analysis of the $d = 1$ case is incomplete, with the incorrect conclusion that the variational theory predicts no phase transition when $d = 1$. The complete expression for $\Delta\mathcal{F}_V(\xi)$ analogous to (39) indeed shows that also for the sG model in $d = 1$ the variational approximation does predict a non-zero temperature below which the physical value of the correlation length is finite.

Finally, for $d = 4$ equation (13) is very similar to that obtained by Saito for the sine-Gordon model

$$\kappa \xi^{-4} = \frac{4\pi^2 V_0}{a_\perp^2} (1 + \pi^4 \xi^4)^{-\frac{T}{16\kappa a_\perp^2}}. \quad (41)$$

Following Saito's analysis for the sine-Gordon model [2], we readily obtain that for $d = 4$ our model has a Kosterlitz-Thouless transition when $T = T_R^{d=4} \equiv 16\kappa a_\perp^2$. The correlation length now diverges as $\xi \sim \exp\{-A/(T - T_R^{d=4})\}$ when $T \rightarrow T_R^{d=4,-}$ (A is a T independent constant).

⁺ The free energy of model \mathcal{H}_0 is \mathcal{F}_0 .

In summary, within the variational approach, our model displays a first order transition for $d < 4$ between a flat phase and a rough phase with the properties of the linear MBE equation. For the marginal dimension $d = 4$ this transition becomes of the Kosterlitz-Thouless type, whereas for $d > 4$ the surface is in the flat phase for all temperature values.

References

- [1] Barabási A L and Stanley H E 1995 *Fractal Concepts in Surface Growth* (Cambridge: Cambridge University Press)
- [2] Saito Y 1996 *Statistical Physics of Crystal Growth* (Singapore: World Scientific)
- [3] Weeks J D 1980 in *Ordering in Strongly Fluctuating Condensed Matter Systems* ed T Riste (New York: Plenum) p 293
- [4] Saito Y 1978 *Z. Phys. B* **32** 75
- [5] Nozières P and Gallet F 1987 *J. Physique* **48** 353
- [6] Sánchez A, Cai D, Grønbech-Jensen N, Bishop A R and Wang Z J 1995, *Phys. Rev. B* **51** 14664
- [7] Kotrla M and Levi A C 1994, *Surf. Sci.* **317** 183
- [8] Moro E, Cuerno R and Sánchez A 1997 *Phys. Rev. Lett.* **78** 4982
- [9] Moro E 1999 *Analytical and Numerical Study of Stochastic Differential Equations: Applications to Statistical Mechanics* Ph. D. thesis (in Spanish: Universidad Carlos III de Madrid)
- [10] Ruiz-Lorenzo J J, Moro E, Cuerno R and Sánchez A 1999 preprint
- [11] Nelson D R 1982 *Phys. Rev. B* **26** 269
- [12] Strandburg K J 1988 *Rev. Mod. Phys.* **60** 161
- [13] Kleinert H 1989 *Gauge Fields in Condensed Matter* (Singapore: World Scientific)
- [14] Prestipino S and Tosatti E 1999 *Phys. Rev. B* **59** 3108
- [15] Janke W and Kleinert H 1986 *Phys. Lett. A* **114** 255
- [16] Janke W and Kleinert H 1990 *Phys. Rev. B* **41** 6848
- [17] Janke W and Toussaint D 1986 *Phys. Lett. A* **116** 387
- [18] Bruce D A 1985 *Mater. Sci. Forum* **4** 51
- [19] Strandburg K J, Solla S A and Chester G V 1983 *Phys. Rev. B* **28** 2717